

Two-way coupled fluid-structure interaction of gas-liquid slug flow in a flexible riser: small-scale experiments and simulations

J. Vieiro^{1*}, A. Akhiartdinov¹, S. Sævik², C.M. Larsen² and O.J. Nydal¹

¹Department of Energy and Process Engineering, Norwegian University of Science and Technology, Trondheim, 7491, Norway.

²Department of Marine Technology, Norwegian University of Science and Technology, Trondheim, 7491, Norway.

*Address all correspondence to Joaquin Vieiro E-mail: joaquin.vieiro.medina@ntnu.no

Abstract

Flexible risers might be subject to large pressure and density fluctuations when transporting multiphase mixtures as different flow pattern may take place. Those fluctuations might induce large forces on the structure which in turn may modify the global geometry of the riser. In this paper, results from one-way and two-way coupled fluid-structure simulations are compared against small scale experiments of a flexible lazy wave riser transporting gas-liquid flow. Different gas flow rates are tested in order to obtain a range of slug frequencies. Predicted values of pipeline pressure, top tension and riser displacement are compared with experimental data. The numerical prediction of the coupled behavior shows fairly good agreement with the experiments, having bias from 5 to 25% in slug frequency.

Keywords: Slug flow, dynamic response, flexible riser, fluid-structure interaction.

1. Introduction

Flexible risers have been installed since the early 70's. This kind of pipe allows permanent connection between a floating support vessel and subsea installations even when large vessel motions take place. Flexible risers have been installed in several configurations including lazy S and lazy wave shown in Figure 1(a) and (b) respectively. Both configurations share features like upper and lower limbs as well as sag and hog bends as presented in Figure 1. The main difference between these two configurations is that in the S configuration there is a subsea buoy or a fixed subsea structure, while in the wave configuration the riser is fitted with distributed weight and buoyancy modules along parts of its length (4Subsea, 2017).

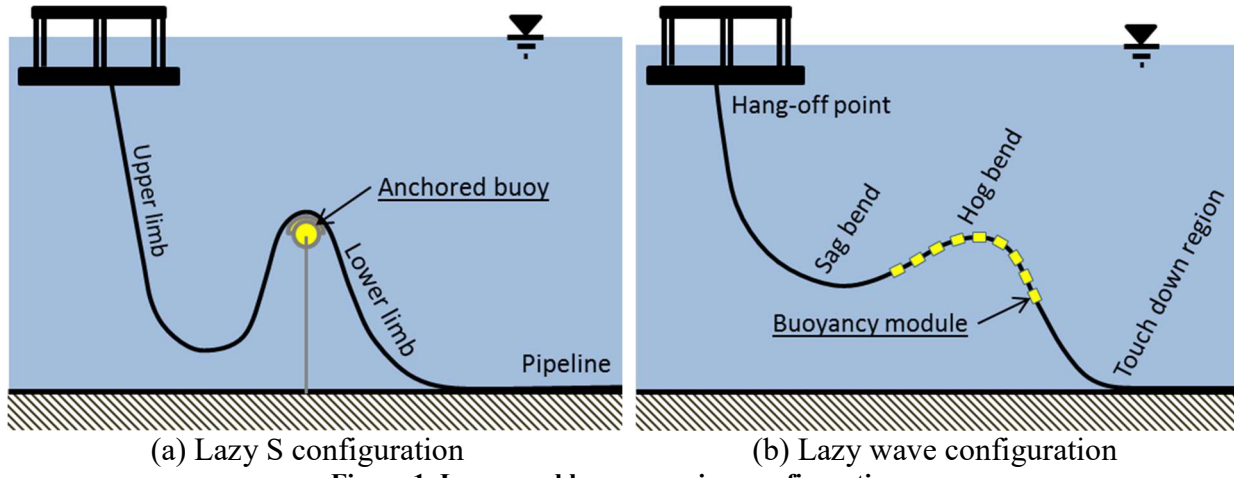


Figure 1. Lazy s and lazy wave riser configurations

One of the disadvantages of using flexible risers is that the configuration is sensitive to changes in the internal fluid density (4Subsea, 2017). This topic is discussed in the present document.

Gas-liquid flow in rigid S-shaped risers has been experimentally studied, among others by:

Tin (1991) studied severe slugging on lazy S and steep S riser configurations as well as free-hanging catenary shape. He found some differences on the severe slugging behavior on s-shaped systems compared with classical severe slugging in vertical risers. He also identified several severe slugging and unstable flow regions, including: Classical severe slugging, unstable liquid column without liquid backup, and continuous gas penetration.

Tin and Sharshar (1993) classified the severe slug cycle depending on the blowout initiation mechanisms (Pipeline gas penetration, trapped gas penetration, intermediate cycle in the lower limb, and no liquid production nor liquid build up in the pipeline).

Nydal et al. (2001) classified the severe slugging phenomena in two types: the first one involving full blockage of liquid in the first bend, and the second one having continuous gas penetration through the same bend at variable rate during the cycle.

Montgomery and Yeung (2002) studied the influence of separator pressure in the stability of severe slugging as well as the liquid production during unstable flow. They found that the severe slugging region shifts to lower gas velocity as pressure increases, and that two liquid production peaks occur during a gas blow out.

Yeung and Tchambak (2003) conducted three phase flow (air-water-oil) experiment in an s-shaped riser. They observed that all the different flow behaviors from air-water two-phase flow were also found in three-phase flow.

Kjeldby and Nydal (2013) compared three-phase oil-water-gas flow simulation with experiments. The numerical model was based on a hybrid slug capturing and slug tracking formulation. Pressure amplitude and slugging period were well reproduced in simulation results.

Li et al. (2013) carried out a series of experiments with a wide range of gas and liquid flow rates and four pipeline inclination angles from -2° to -5° . They presented flow pattern maps for each pipeline inclination and concluded that the region of severe slugging expands to higher flow rates as the pipeline angle decreases.

Diaz et al. (2013) and Diaz et al. (2014) studied the influence of liquid viscosity on the stability region of gas-liquid flow. They found that stable flow is obtained for lower gas velocities as the viscosity increases.

Park and Nydal (2014) compared OLGA simulations with experimental results of an S-shaped riser conveying air-water flow. They concluded that simulation results compare quite well with the experimental measurements.

Early studies incorporating slug flow on the dynamic response of flexible s-shaped risers involved mathematical functions to describe a simplified internal flow behavior where slugs enter and leave the riser with specified velocity and frequency. Flow pattern changes were neglected as well as slug growth and decay. Among those studies are the following:

Patel and Seyed (1989) presented a derivation of the governing equations of flexible risers in two dimensions including internal and external hydrostatic pressure and internal slug flow effects. The internal flow was described by periodic functions in time and space. They showed that dynamic slug flow can subject the riser to large fluctuating tension forces.

Seyed and Patel (1992) showed simulation results for combined waves, vessel motion and slug flow effects on a lazy S riser. Induced motions by wave and vessel motion or slug flow were not so significant, but the combined effect exhibited considerably larger displacement.

Gundersen et al. (2012) studied a lazy S riser under environmental and slug flow loads. Slug parameters such as density, length, velocity and period were tuned in order to describe ROV observations of the actual riser. In a case study, they demonstrated that slugging can reduce the riser fatigue life significantly.

A few coupled two-way fluid-structure interaction studies regarding slug flow and flexible risers have been published in the last decade. This way of analysis performs numerical solution for both pipe flow and structural response, where relevant forces and geometry changes are communicated between the physical phenomena in order to include the influence of the flow dynamics in the structural response and vice-versa.

Ortega et al. (2012) studied the influence of slug flow in the dynamic response of a lazy wave riser using a feedback connection between a structural dynamic software and a multiphase flow software by means of high level architecture. Ortega et al. (2017) used an improved structural model in order to predict the influence of waves and slugs in the movement of a catenary riser.

Vieiro and Nydal (Submitted for publication) presented a standalone coupled model for coupled fluid-structure interaction in flexible pipes conveying multiphase flow. They compared numerical results with experimental data regarding air-water two-phase flow in a floating hose. The model was also tested on a two-phase flow garden hose instability case (Vieiro et al., 2014) and on a case

with slug flow induced by buoyancy elements attached to a flexible riser which had collapsed and resting on the seabed (Vieiro et al., 2016) (similar as for a blow-out case in the Mexico Gulf).

This study presents small scale experiments on gas-liquid flow in a submerged, flexible, lazy wave shaped riser. The base concepts for a two way coupled flow-structure model is described and simulations are compared with experimental results.

2. Numerical model

The two-way coupled model used in this research consists of a lumped mass model for structural dynamics (with similarities to the scheme described by Ghadimi (1988)) and a 1D slug tracking and capturing model for multiphase flow in pipes (Nydal, 2012). The models are coupled using explicit domain-decomposition method, where both models are solved independently and information is exchanged during certain instants in order to include the influence of one phenomenon into the other.

Figure 2 shows an example of the decomposition of a physical system in structural and fluid domains. Figure 2(a) presents a sketch of a hog bend section of a flexible riser, where a cut on the pipe wall and buoyancy sections is made in order to show the internal flow. Table 2(b) and (c) show graphical representations of the structural and fluid domains.

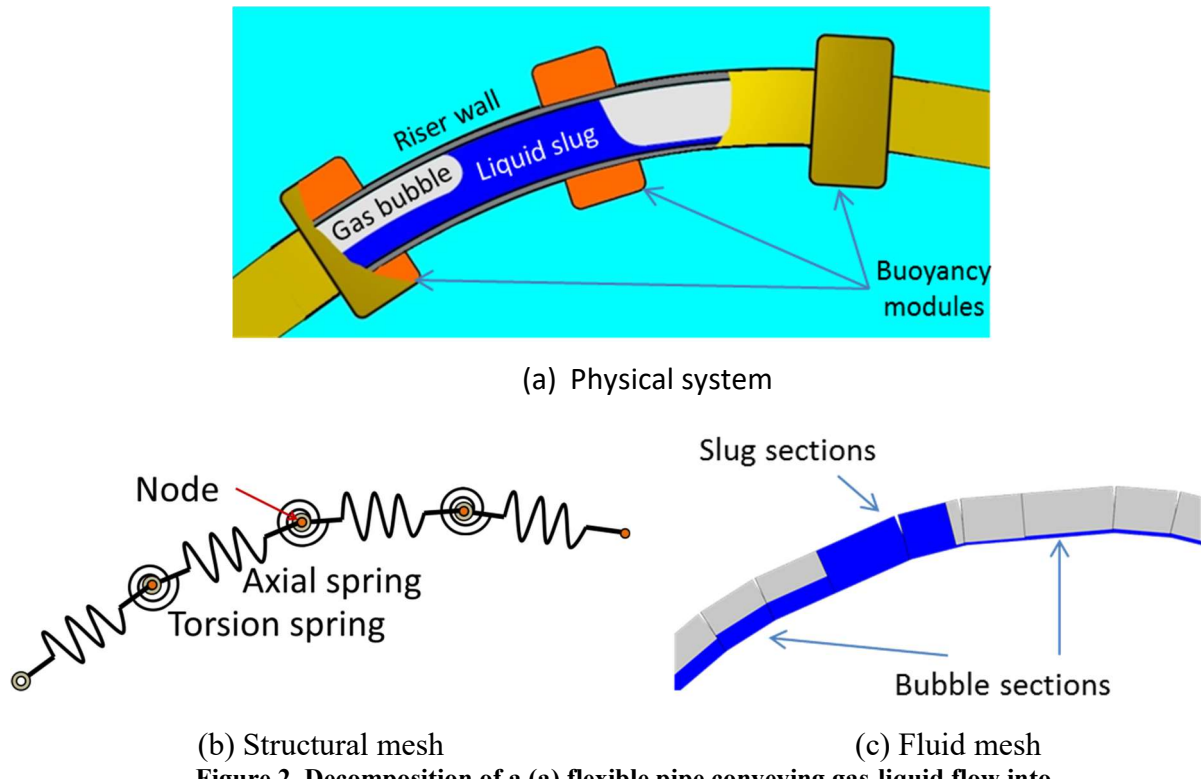


Figure 2. Decomposition of a (a) flexible pipe conveying gas-liquid flow into (b) structural domain and (c) fluid domain.

On the structural domain, the pipe is divided in straight elements having a node on each end. Axial and bending stiffness are modeled as springs and dampers. Figure 2(b) shows an example of structural mesh where dampers are not shown for the sake of simplicity. Internal and external forces are applied on the nodes. Forces resulting from the presence of internal flow, including fluid

weight, force on bends due to changes in flow direction and Coriolis forces. The feedback from the pipe structure to the flow is in the inclination of flow grid.

The internal multiphase flow is modelled by using a slug tracking and capturing formulation based on the two-fluid model. The fluid domain is divided in cells as shown in Figure 2(c). The mesh is dynamically updated following the structural displacements as well as fluid distribution. Two types of fluid cells are used here: Bubble cells and slug cells. Bubble cells are used where the liquid volume fraction is below a pre-established liquid holdup value, and are solved using a two fluid model on an Eulerian formulation. Liquid slugs are created when the minimum liquid holdup condition is fulfilled, and the slugs cells are tracked using a Lagrangian formulation with an integral momentum equation over the slug length. Cells neighboring slugs might be split or merged in order to satisfy maximum and minimum section length conditions as the slugs propagate along the domain. Figure 2(c) shows an example of a domain having both slug and bubble sections.

As structural and fluid domains have different time and space grids, feedback criteria and mapping algorithms in space are needed. As the structural solver time steps are always shorter than fluid time steps, it is set that information between the domains is exchanged after every fluid solver time step. Flow variables on fluid cells are mapped on the pipes using weighted averages of the fluid cells spanning each pipe depending on the overlapping length. The fluid cells are updated following the pipe angle variations. Figure 3 outlines the calculation procedure.

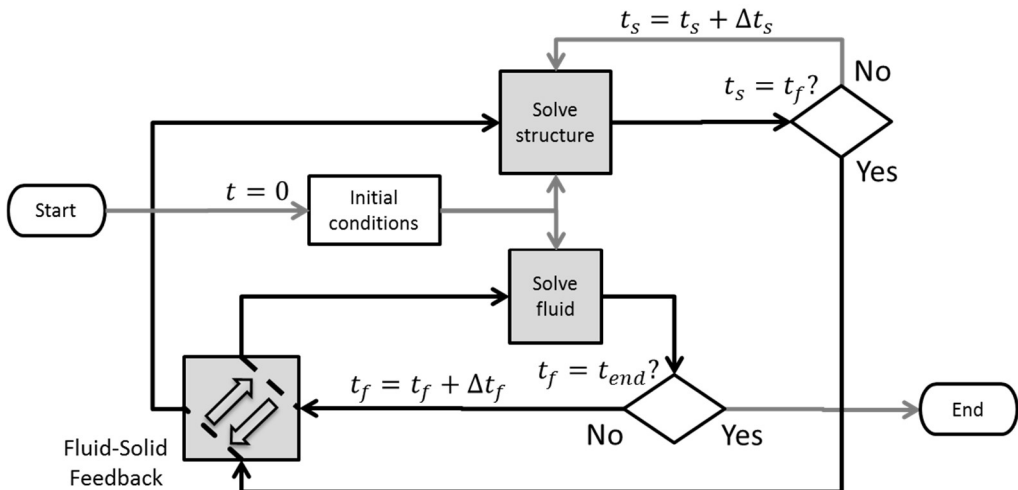


Figure 3. Simplified algorithm for coupled model.

One-way coupled simulations are carried out by omitting the fluid cell angle updates.

3. Experimental setup

The small-scale flexible riser is made using a silicon hose with the properties in Table 1.

Table 1. Mechanical characteristics of pipeline-riser system

Internal diameter (mm)	15.3
Wall thickness (mm)	3.4
Linear mass density (kg/m)	0.23
Modulus of elasticity (MPa)	6.0

The modulus of elasticity was determined by tuning to the static shape of the hanging riser. In order to establish the lazy wave shape, ballast and buoyancy modules are needed. A stainless steel chain is fixed along the riser in order to add distributed ballast, without changing the bending stiffness. Marks and buoyancy modules are fixed on the riser at the locations specified on Figure 4(a) and (b). Eight marks are set for visual tracking purposes.

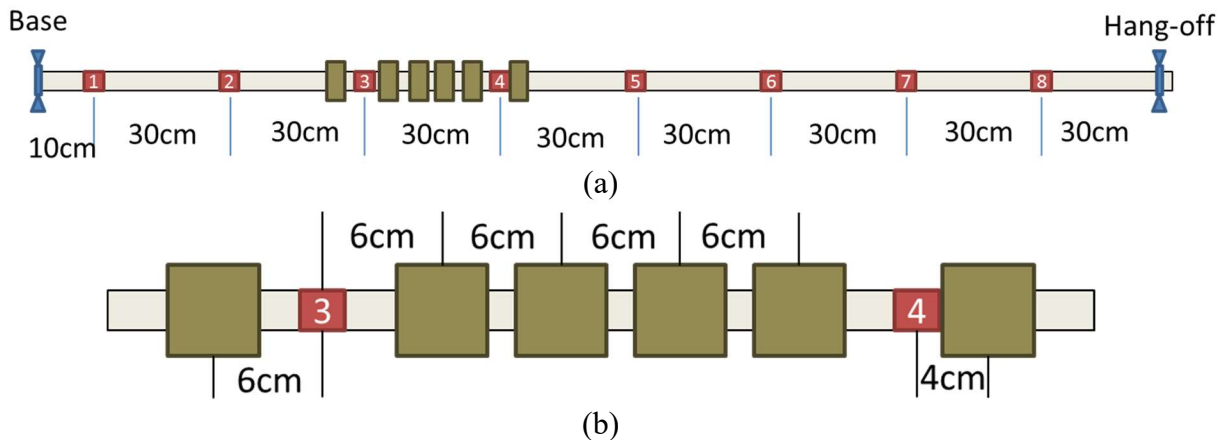


Figure 4. Location of (a) marks and (b) buoyancy sections along the riser.

A 45° circular section is removed from each buoyancy module in order to avoid interference with the ballast chain. Figure 5(a) and (b) outlines the buoyancy and ballast geometry respectively.

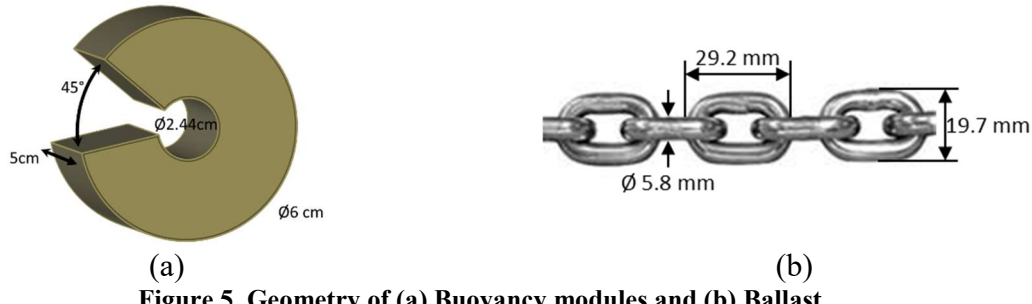


Figure 5. Geometry of (a) Buoyancy modules and (b) Ballast.

The air water flow is obtained by using a water pump and a compressor. An air buffer tank of 8160 cm^3 is installed in order to increase compressibility in the system. The hose with attachments is submerged in a water tank and fixed as shown in Figure 6. The riser base is fixed on an inclined surface at 1.52 m below the mixing point level. Downhill inclination is imposed to the hose between the mixing point and the riser base in order to induce stratified flow. The outlet of the riser is fixed to a load cell in order to measure top tension. The hose section between the riser base and the hang-off is allowed to move, whereas the remaining was fixed.

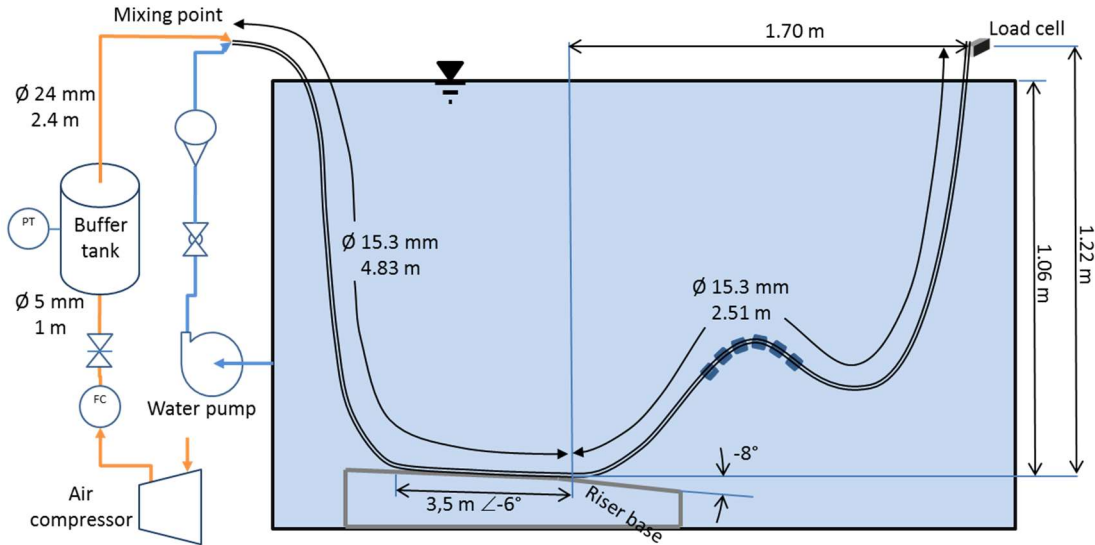


Figure 6. Experimental setup

The fundamental frequencies of the riser system fully filled with air or water are found to be 0.32 Hz and 0.52 Hz respectively.

The water flow rate is set to 50 l/h (liters per hour) and different values of air flow rate from 2 to 12 nl/m (normal liters per minute) are studied. The displacements of the marks along the hose are recorded using a video camera located outside the tank directly in front of the test section. Data such as buffer tank pressure and hang-off force are logged during the experiments.

4. Numerical setup

The structural domain is discretized in elements of different lengths. Downstream of the riser base, the flexible section is divided into 55 elements no larger than 5cm. The geometry of the fixed section and riser are summarized in Table 2 and Table 3.

Table 2. Geometry of the fixed domain

Pipe number	Internal Diameter (cm)	Angle (°)	Length (m)
1	0.5	90	1.00
2	20	90	0.26
3	2.4	90	0.69
4	1.525	-15.1	0.881
5	1.525	-66.5	1.20
6	1.525	-5	2.10
7	1.525	-6	0.15
8	1.525	-7	0.15
9	1.525	-8	0.30
10	1.525	-8	0.05

Table 3. Geometry of the flexible domain

Pipe number	External Diameter (cm)	Stress free length (cm)
11	2.17	2
12-14	2.17	3
15-25	2.17	5
26,28,30,32,34,36	5.80	5
27,29,31,33,35	2.17	2
37-65	2.17	5

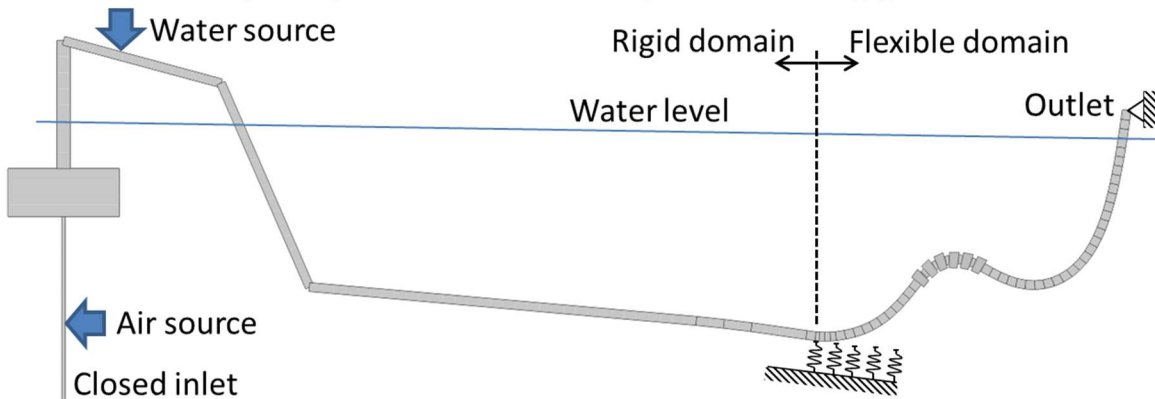
The buoyancy modules are modeled as cylindrical sections having the same volume as the actual modules presented on Figure 5. Drag and added mass coefficients are adjusted in order to account for the effect on a cylinder of 6 cm diameter (Neglecting the effects of the missing 45° sector). The influence of drag and added mass by the presence of the ballast chain is neglected. The values of added mass and drag coefficients are displayed in Table 4.

Table 4. Drag and added mass coefficients along the flexible domain

	Bare riser	Buoyancy section
Normal drag coefficient (-)	1.1	1.1
Axial drag coefficient (-)	0.1	0.2
Added mass coefficient on normal direction (-)	1.0	1.2
Added mass coefficient on axial direction (-)	0.0	0.0

All the nodes along the pipeline are fixed to ground, as well as the riser hang-off node. The out of plain motion is suppressed so that the riser motion occurs in the x-y plane. The ground stiffness is set to 100 kN/m.

Air and water sources are supplied as shown in Figure 7. The inlet is kept closed and the outlet pressure is set to atmospheric pressure. The inside roughness of all the pipes is set to 4.5e-2 mm.

**Figure 7. Boundary conditions for fluid and structural domains**

The maximum and minimum length of fluid sections is set using the values in Table 5.

Table 5. Maximum and minimum length of fluid sections

	Location	Maximum length (cm)	Minimum length (cm)
Bubble sections	Rigid domain	40.0	1.0
	Flexible domain	4.0	1.0
Slug sections	Whole domain	∞	0.5

The maximum fluid and structure time steps are set to 1e-2 and 1e-4 s respectively. All the simulations are run for 400 s.

The natural frequencies for air filled and liquid filled riser are obtained by mean of dynamic simulations without solving the internal flow. Frequencies of 0.26 Hz for air filled and 0.37 Hz for water filled conditions are obtained. Better natural frequencies would be predicted by improving the normal added mass coefficient on the pipe with buoyancy modules and including ballast chain effects.

5. Results

No appreciable differences were observed between one-way or two-way coupled simulations, meaning that the variations in the riser configuration do not have a significant impact on the flow dynamic. For simplicity only the two-way coupled results will be presented.

It is observed that buffer tank pressure, hang-off force and riser displacement time series share a common dominant frequency for each experiment. The experimental and numerical dominant frequencies for all the studied cases are presented on Figure 8. In the worst case (4 nl/m), the dominant frequency is underpredicted by 24%.

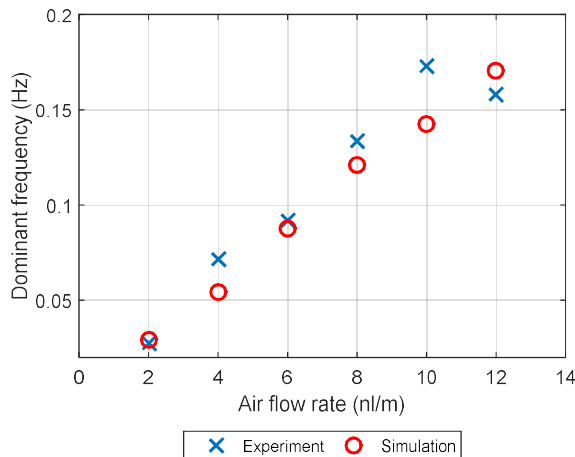


Figure 8. Dominant frequency vs air flow rate for experiments and simulations

Three of the six cases showed in Figure 8 will be discussed in the following. The Cases will be described using the flow patterns classification presented by Nydal et al. (2001).

5.1. Case 2 nl/m. Terrain induced slugging type I

In Severe Slugging type I, the liquid forms a complete blockage on the first bend. This case is characterized by well-defined low frequency buffer pressure/top tension/riser displacement time series. The buffer tank pressure oscillates between 1kPa and 12kPa (Hydrostatic pressure at the

bottom of a water column of the riser height). Figure 9 shows the experimental and numerical pressure time series for this case. Some features may be observed in the pressure time series of Figure 9, and will be explained with help of simulation results on Figure 10(a) to (i).

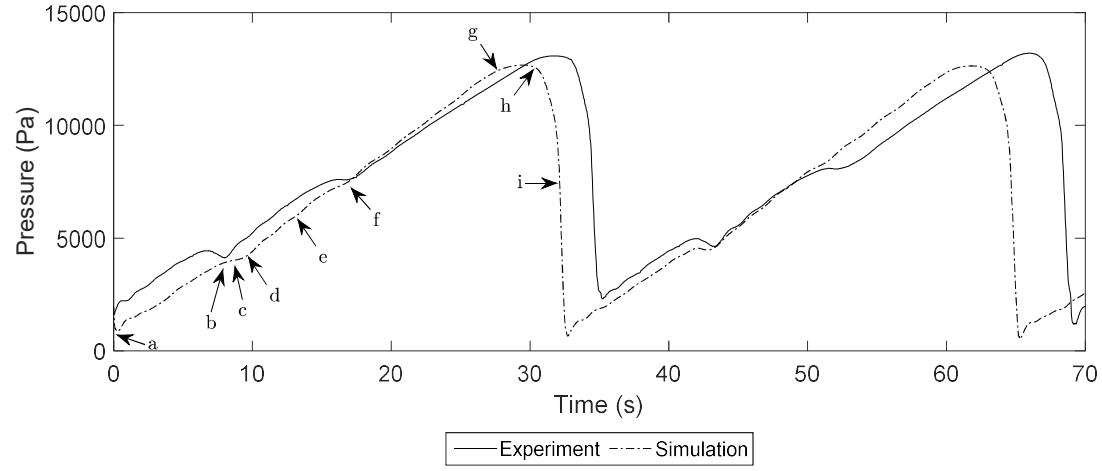


Figure 9. Experimental and numerical buffer pressure time series for 2 nl/m

The minimum pressure takes place after the gas blowout from the previous cycle, and two small slugs containing the remaining liquid block at touchdown and hog bends as in Figure 10(a). The first peak around $t=6.7\text{s}$ occurs just when the slug in the lower limb reaches the top of the hog bend as in Figure 10(b). As the liquid film is created in the downward section, air from the trapped bubble is pushed through the sag bend producing a small pressure drop (Figure 10(c)). The slug tail reaches the lower bend and a short stage of gas penetration starts (Figure 10(d)). The hog bend is completely occupied by gas, and pressure increase as the slug front in the lower limb rises (Figure 10(e)). The slug in the lower limb grows until the top of the hog bend is reached again, and more air is pushed through the sag bend (Figure 10(f)). The slugs in the upper and lower limbs grow, reaching the top of the riser and the pipeline (Figure 10(g)). The slug tail is pushed beyond the touchdown bend followed by gas blowout (Figure 10(h)) and Figure 10(i)).

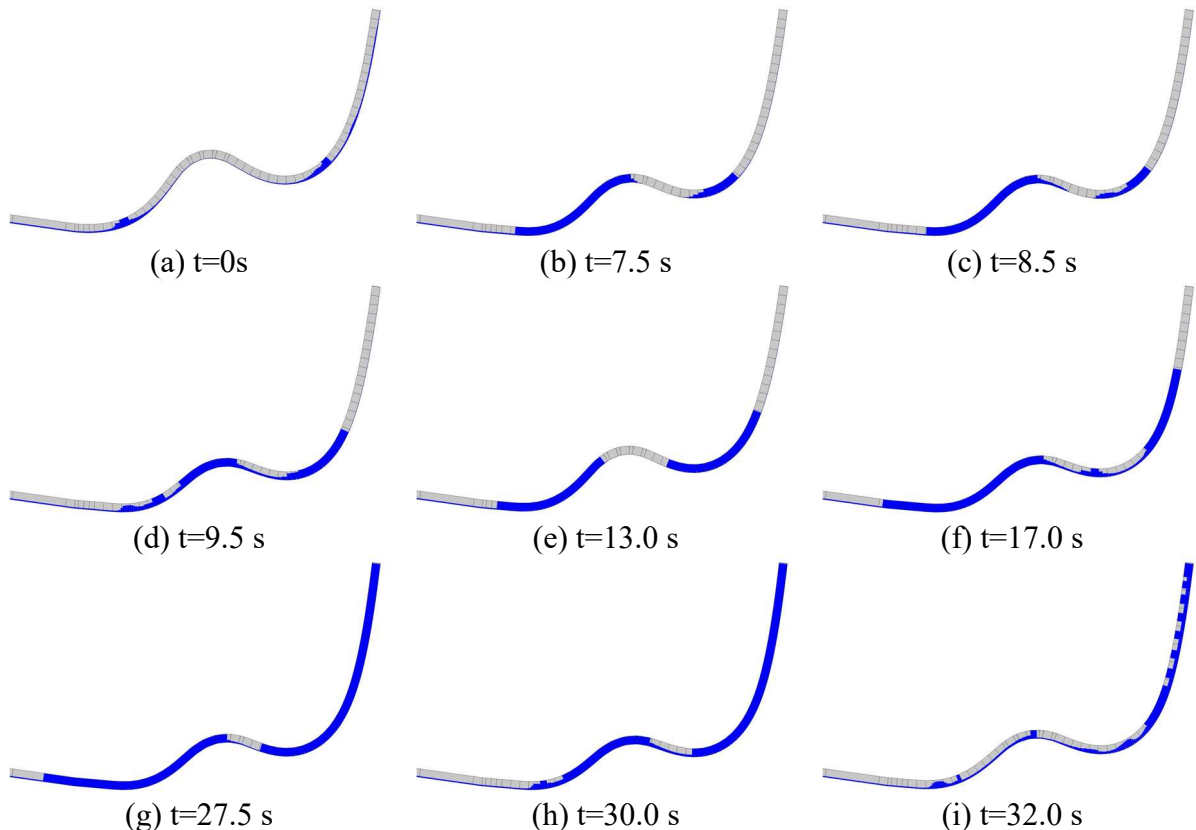


Figure 10. Snapshots of simulation results showing different stage of severe slugging cycle.
(Pipe diameter scaled by 3)

The riser displacement envelopes and vertical displacement of mark 4 are shown in Figure 11 and Figure 12, respectively. It is observed that the displacement of the hog bend recorded during the experiment (Figure 12) exceeded 8 external riser diameters, while the simulation predicted a displacement of 11 riser diameters.

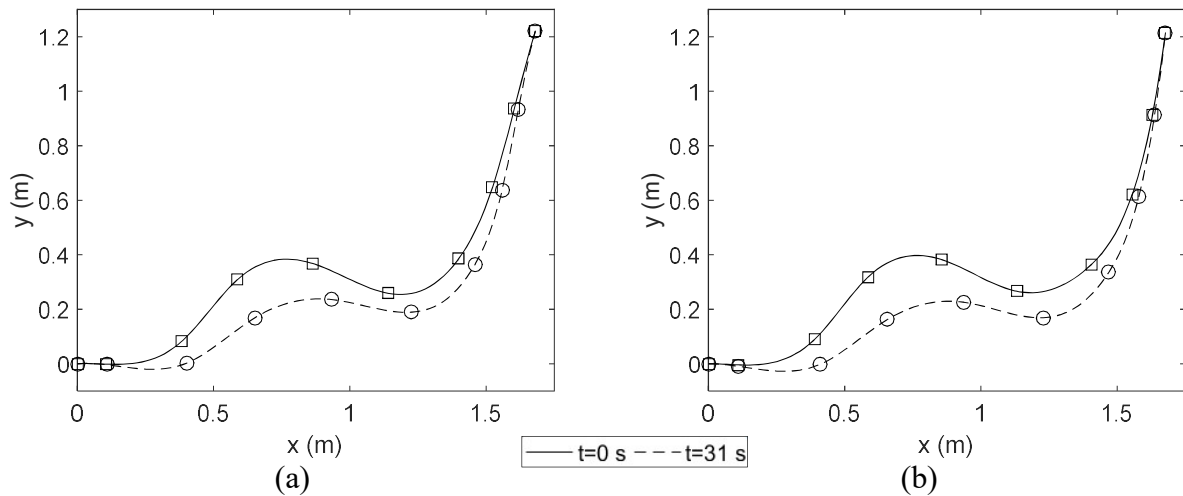


Figure 11. Riser displacement for 2 nl/m at $t=0$ and $t=31 \text{ s}$ for (a) Experiment and (b) Simulation.

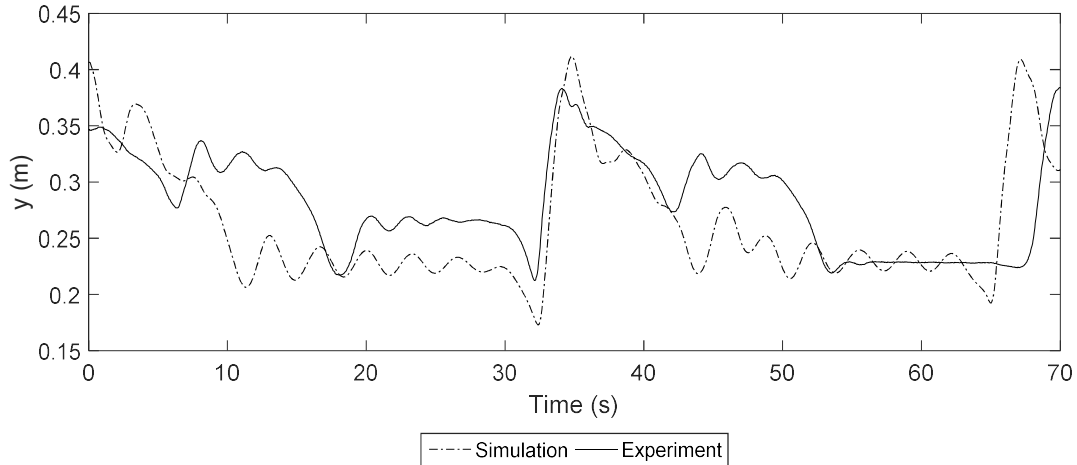


Figure 12. Vertical displacement of mark 4.

The riser top tension increased as the pipe is filled with water and presented a sharp reduction as the riser is filled with gas during the blow out as shown in Figure 13. The measured top tension presented a narrow peak of about 1 s and the simulation predicted a wider peak of 4 s.

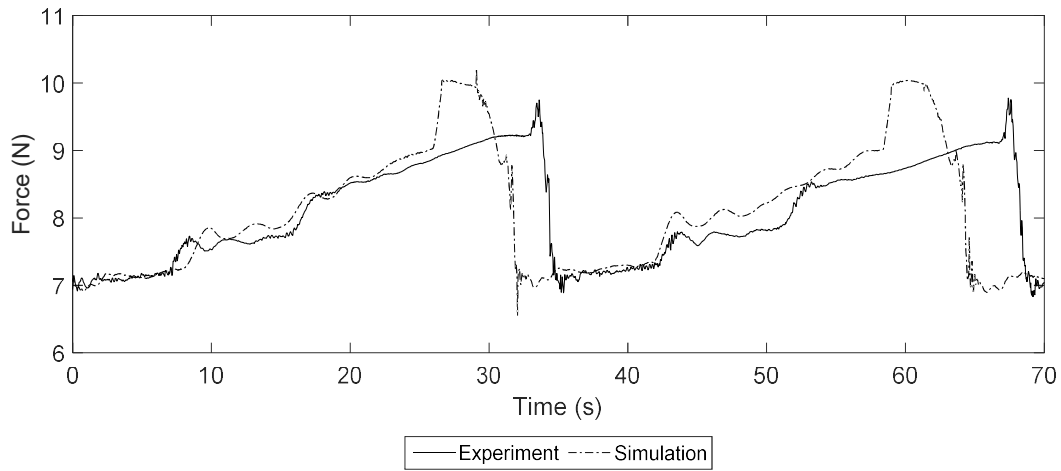


Figure 13. Experimental and numerical top tension time series for 2 nl/m

5.2. Case 6 nl/m. Terrain induced slugging type II

In Severe Slugging type II, gas always penetrates the bend, but at varying flow rates. The experiment and simulation show a cyclic behavior with two characteristic stages: in the first one, slugs are generated in the riser base and pushed downstream to the sag bend. In the second stage, a new slug is created in the riser base and both slugs are expelled from the riser.

It is observed during the experiment that some liquid is produced on first stage described above. This is not reproduced by the model as the liquid reaches the top of the riser only during the second stage.

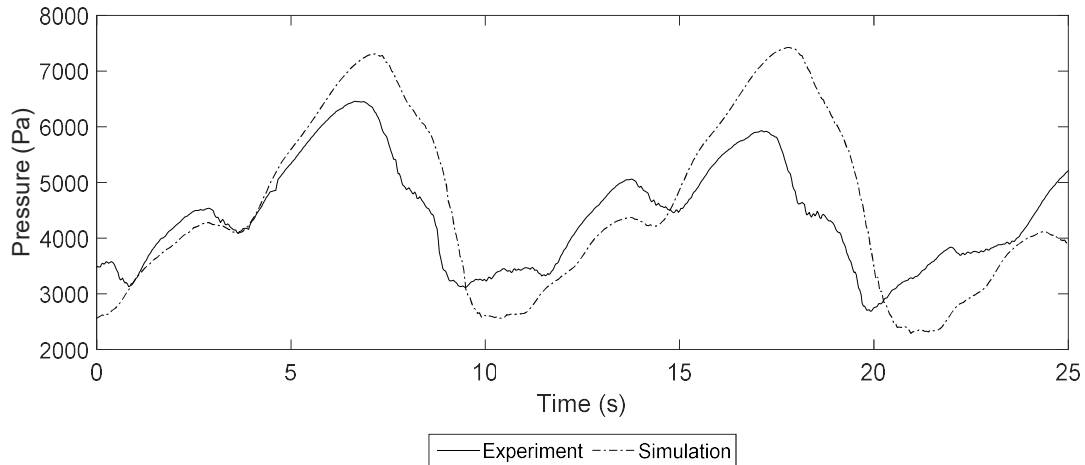


Figure 14. Experimental and numerical buffer pressure time series for 6 nl/m

Figure 15 presents shorter slugs compared with the previous case. The slugs in the upper limb on Figure 15(a) and (b) will eventually break up and flow back to the sag bend until the blow out take place as in Figure 15(c).

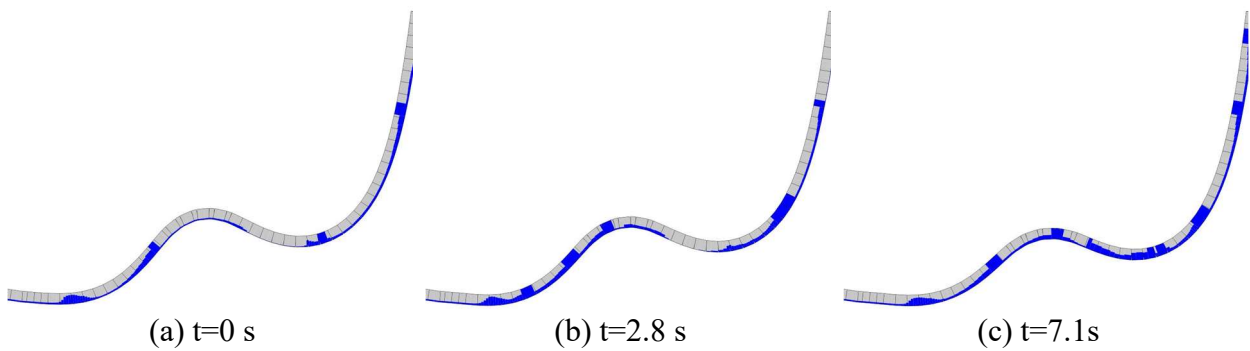


Figure 15. Snapshots of riser geometry and holdup for case 6 nl/s.
Diameter scaled by three.

The predicted riser displacement is considerably overestimated for this case as observed on Figure 16. This might be expected as the mean density inside the riser is higher due to the larger accumulation of liquid within it.

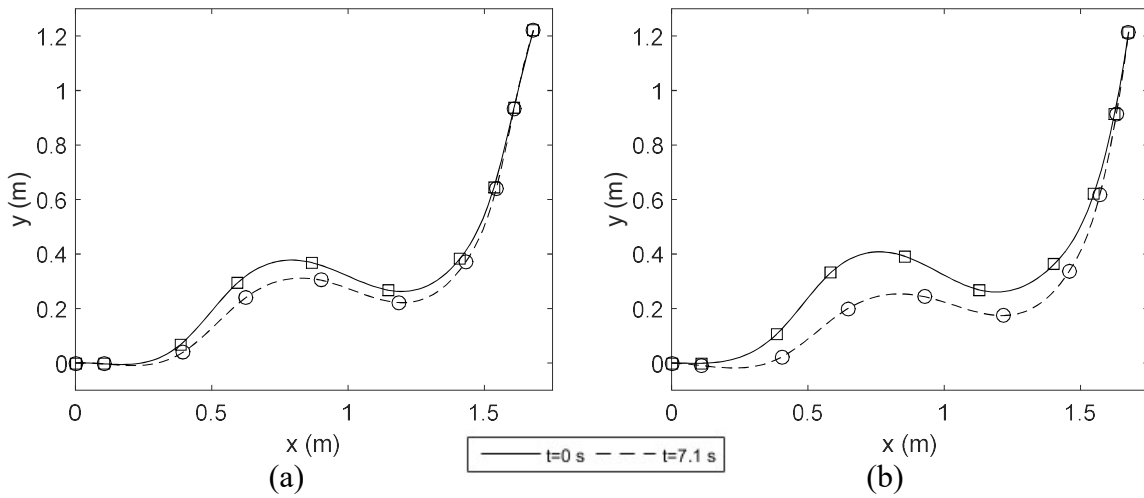


Figure 16. Riser displacement for 6 nl/m at different instants for (a) Experiment and (b) Simulation.

A high frequency component is observed on the top tension time series in Figure 17.

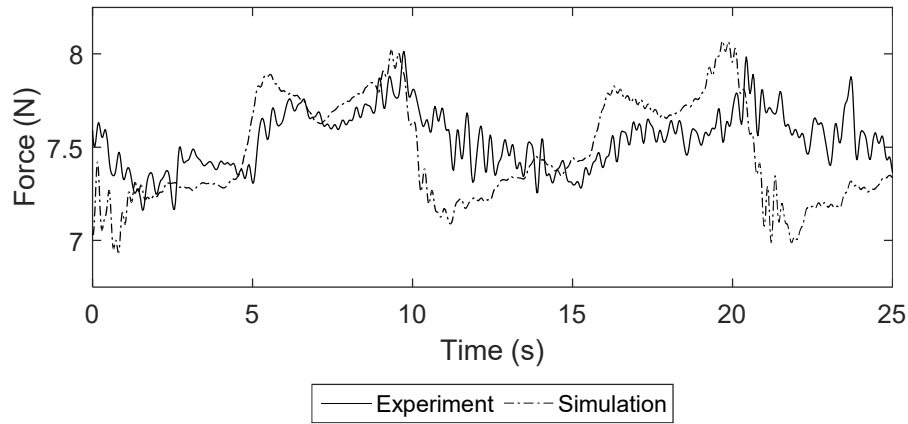


Figure 17. Experimental and numerical top tension time series for 6 nl/m

5.3. Case 10 nl/m. Stable flow

Short slugs are observed in the experimental and simulation results for this case. Irregular low amplitude oscillations in the pressure time series are observed in both the experimental and simulated results as presented in Figure 18.

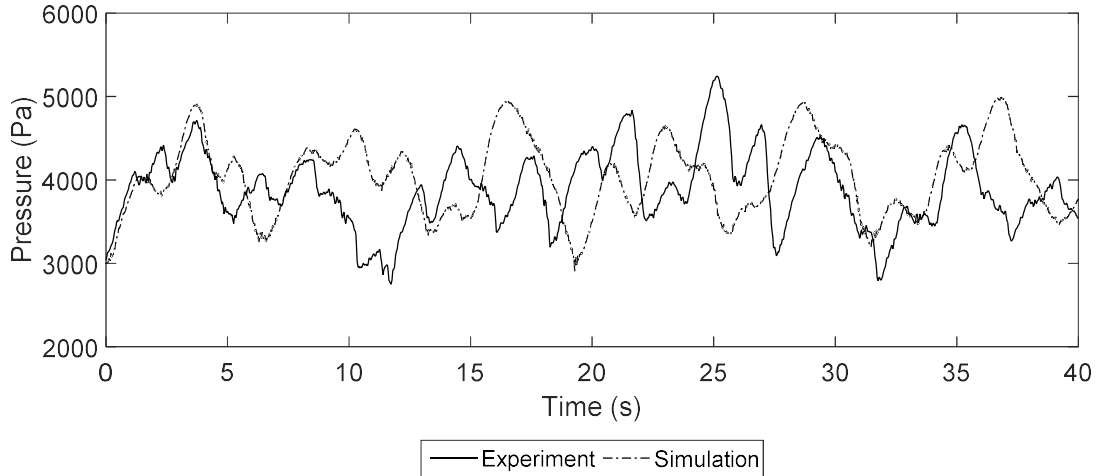


Figure 18. Experimental and numerical buffer pressure time series for 10 nl/m

The power spectral density (PSD) estimate by Welch's method is calculated and plotted on Figure 19. It is observed that the experimental pressure time series have several significant contributions from frequencies between 0.035 to 0.58 Hz, with dominant frequency of 0.17 Hz. The power spectral density plot of the pressure time series from the simulation shows a dominant frequency of 0.14 Hz and a secondary peak at 0.30 Hz.

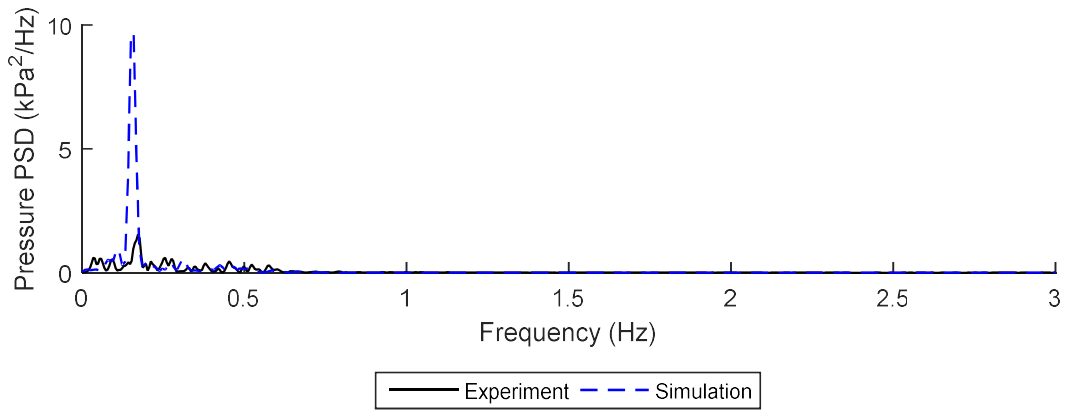


Figure 19. Power spectral density estimate of pressure for case 10 nl/m

Figure 20(a) and (b) present the riser displacement for case 10 nl/m. It is observed that the displacement for this case is considerably less significant than the previous cases.

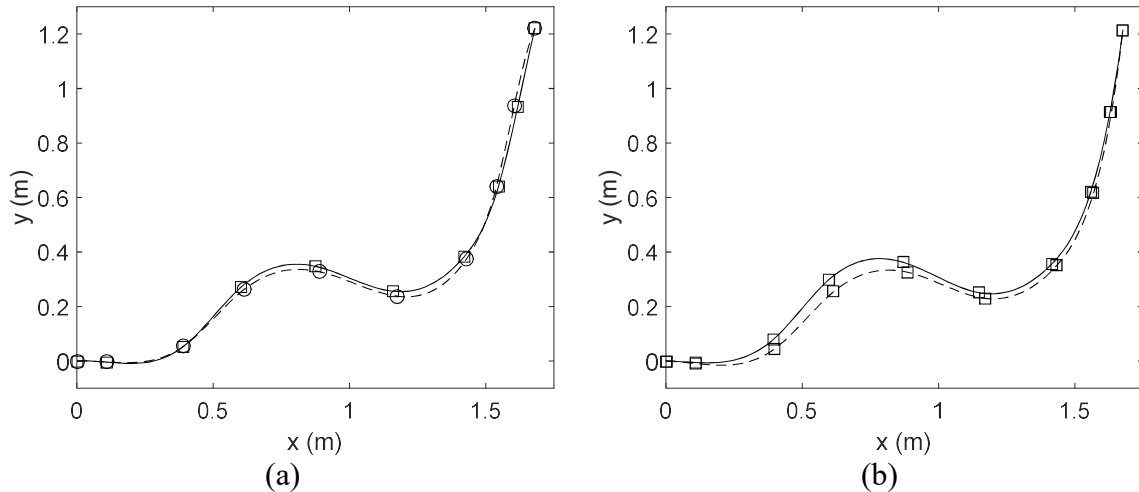


Figure 20. Riser displacement for 10 nl/m at different instants for (a) Experiment and (b) Simulation.

Figure 21 shows a representative liquid holdup distribution for the simulation. It is observed that slugs are created on the riser base and sag bend as for the case with 6 nl/m. Most of the slugs created on the riser base reach the hog bend, and all of those reaching that point are transformed into stratified flow before reaching the sag bend. Slugs are created just downstream of the sag bend and pushed upward. Not all of those slugs reach the outlet, as some of them are transformed to stratified flow that flows back to the sag bend.

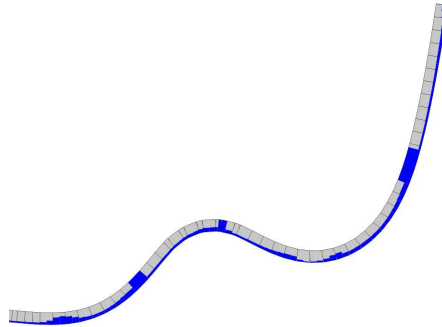


Figure 21. Snapshot of riser geometry and holdup for case 10 nl/s.
Diameter scaled by three.

The force time series presented even more complex behavior as shown on Figure 22. Spectral analysis shows minor contributions of frequencies above 2 Hz as presented in Figure 23.

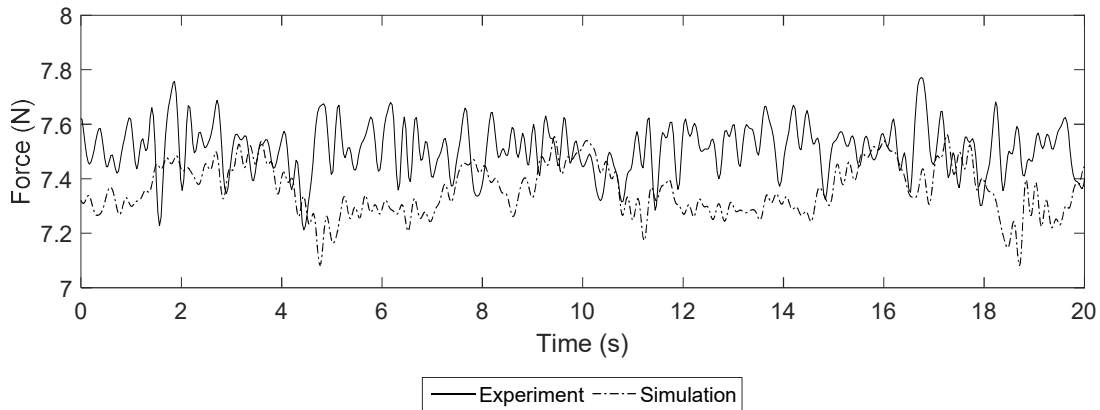


Figure 22. Experimental and numerical top tension time series for 10 nl/m

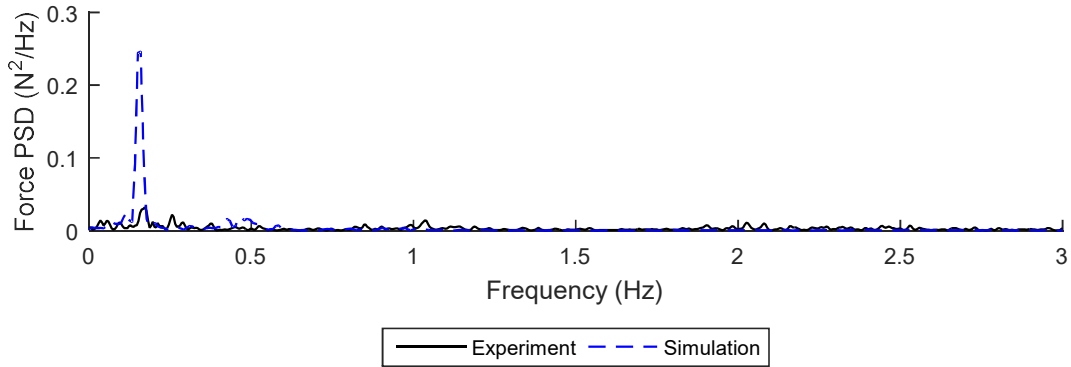


Figure 23. Power spectral density estimate of top tension for case 10 nl/m

6. Conclusions

A test case consisting of a small scale flexible riser conveying gas-liquid flow is successfully reproduced by using a coupled fluid-structure interaction model. Two-way coupled simulations are not found necessary for the presented test case since the differences between one-way and two-way coupled simulations are found negligible. Six different gas flow rates are tested and three among those are explained using pressure and top tension time series as well as riser displacement. It is observed that the internal flow dynamic and the pipe displacements are quite well reproduced for terrain induced slugging type I (full riser blockage at first bend) and stable flow. The case involving terrain induced slugging type II (partial riser blockage at first bend) shows qualitatively same trends, but larger deviations from experimental values.

Acknowledgements

Project / research funded by VISTA - a basic research program and collaborative partnership between The Norwegian Academy of Science and Letters and Statoil.

References

- 4Subsea. (2017). Flexible Pipe Systems. In D. Fergestad & S. A. Løtveit (Eds.), *Handbook on design and operation of flexible pipes* (2017 ed.). Trondheim: SINTEF Ocean.

- Diaz, M. J. C., Akselsen, A. H., & Nydal, O. J. (2013). *Experiments on severe slugging in a S-riser system with viscous liquids*. Paper presented at the 8th International conference on Multiphase Flow, Jeju, Korea.
- Diaz, M. J. C., Khatibi, M., & Nydal, O. J. (2014). *Severe Slugging With Viscous Liquids: Experiments and Simulations*. Paper presented at the 9th North American Conference on Multiphase Technology, Banff, Canada.
- Ghadimi, R. (1988). A simple and efficient algorithm for the static and dynamic analysis of flexible marine risers. *Computers & Structures*, 29(4), 541-555. doi:[https://doi.org/10.1016/0045-7949\(88\)90364-1](https://doi.org/10.1016/0045-7949(88)90364-1)
- Gundersen, P., Doynov, K., Andersen, T., & Haakonsen, R. (2012). *Methodology for Determining Remnant Fatigue Life of Flexible Risers Subjected to Slugging and Irregular Waves*. Paper presented at the 31st International Conference on Ocean, Offshore and Arctic Engineering, Rio de Janeiro. <http://dx.doi.org/10.1115/OMAE2012-83412>
- Kjeldby, T. K., & Nydal, O. J. (2013). A Lagrangian three-phase slug tracking framework. *International Journal of Multiphase Flow*, 56, 184-194. doi:<https://doi.org/10.1016/j.ijmultiphaseflow.2013.05.013>
- Li, N., Guo, L., & Li, W. (2013). Gas–liquid two-phase flow patterns in a pipeline–riser system with an S-shaped riser. *International Journal of Multiphase Flow*, 55, 1-10. doi:<https://doi.org/10.1016/j.ijmultiphaseflow.2013.04.003>
- Montgomery, J. A., & Yeung, H. C. (2002). The Stability of Fluid Production From a Flexible Riser. *Journal of Energy Resources Technology*, 124(2), 83-89. doi:10.1115/1.1467646
- Nydal, O. J. (2012). Dynamic Models in Multiphase Flow. *Energy & Fuels*, 26(7), 4117-4123. doi:10.1021/ef300282c
- Nydal, O. J., Audibert, M., & Johansen, M. (2001). *Experiments and modelling of gas-liquid flow in S-shaped riser*. Paper presented at the 10th International conference on multiphase production, Cannes.
- Ortega, A., Rivera, A., & Larsen, C. M. (2017). Slug Flow and Waves Induced Motions in Flexible Riser. *Journal of Offshore Mechanics and Arctic Engineering*, 140(1). doi:10.1115/1.4037842
- Ortega, A., Rivera, A., Nydal, O. J., & Larsen, C. M. (2012). *On the Dynamic Response of Flexible Risers Caused by Internal Slug Flow*. Paper presented at the 31st International Conference on Ocean, Offshore and Arctic Engineering, Rio de Janeiro, Brazil. <http://dx.doi.org/10.1115/OMAE2012-83316>
- Park, S., & Nydal, O. J. (2014). Study on Severe Slugging in an S-Shaped Riser: Small-Scale Experiments Compared With Simulations. *Oil and Gas Facilities*, 3(4). doi:10.2118/171559-PA
- Patel, M. H., & Seyed, F. B. (1989). Internal flow-induced behaviour of flexible risers. *Engineering Structures*, 11(4), 266-280. doi:[https://doi.org/10.1016/0141-0296\(89\)90046-1](https://doi.org/10.1016/0141-0296(89)90046-1)
- Seyed, F. B., & Patel, M. H. (1992). *Considerations In Design Of Flexible Riser Systems*. Paper presented at the The Second International Offshore and Polar Engineering Conference, San Francisco, California, USA.
- Tin, V. (1991). *Severe Slugging in Flexible Risers*. Paper presented at the 5th International Conference on Multiphase Production, Cannes, France.
- Tin, V., & Sharshar, M. M. (1993). *An investigation of severe slugging characteristics in flexible risers*. Paper presented at the 6th International Conference on Multiphase Production, Cannes, France.

- Vieiro, J. J., Hemedha, A., & Nydal, O. J. (2014). *Multiphase Flow in Flexible Pipes: Coupled Dynamic Simulations and Small Scale Experiments on Garden Hose Instability*. Paper presented at the Eighth National Conference on Computational Mechanics, MekIT'15, Trondheim, Norway.
- Vieiro, J. J., Hemedha, A., & Nydal, O. J. (2016). *Experimental and Numerical Simulation of two-phase flow and structural dynamic of a collapsed flexible pipe on the seabed*. Paper presented at the International conference on the Advances in Subsea Engineering, Structures and Systems, Glasgow, United Kingdom.
- Vieiro, J. J., & Nydal, O. J. (Submitted for publication). Experimental and numerical study of a flexible floating pipe conveying multiphase flow. *Journal of Fluids and Structures*.
- Yeung, H., & Tchambak, E. (2003). *Three phase flow in an s-shaped riser - some preliminary results*. Paper presented at the 11th International conference on Multiphase 03, San Remo, Italy.